

Evaluation of Modified Fish-Bone Model for Estimating Seismic Demands of Irregular MRF Structures

Amin Haghghat^{1,2}, Ashkan Sharifi^{1,2*}

RESEARCH ARTICLE

Received 23 October 2017; Accepted 27 March 2018

Abstract

This paper evaluates the accuracy of the Modified Fish-Bone (MFB) model for estimating the maximum inter-story drift ratio of irregular moment resisting frame (MRF) structures. To make this model applicable to irregular MRF structures, some modifications are made to the MFB formula. In order to evaluate the accuracy of the MFB model, several irregular frames with different types of irregularities are considered when subjected to different ground motions with different intensities. A local and a global error measure are defined and they are calculated for different frame models subjected to different earthquake records. The effects of different irregularities, ductility demand and frame height on the accuracy of the MFB model are investigated. Based on the results obtained from this evaluation, two simple and effective approaches are suggested to improve the MFB models.

Keywords

irregular moment resisting frame, inter-story drift ratio, modified fish-bone, nonlinear dynamic analysis, seismic demand

1 Introduction

Estimation of seismic deformation demands of a structure is one of the key steps for retrofit and performance-based seismic design (PBSD) of the structure. The most accurate analysis for estimating seismic deformation demands is nonlinear time-history analysis. However, such analysis suffers from the high computational intensity and not practical for day-to-day designs. Thus, researchers are trying to replace it by simplified approximation methods such as linear dynamic analysis or equivalent nonlinear static analysis. The results of such investigations are used by usual rehabilitation guidelines and codes such as FEMA 356 [1] and ASCE 41-13 [2] to introduce some reliable and practical equivalent approximation methods for day-to-day analyses and designs. However, for irregular structures in which the redistribution of internal forces is high, and the effects of higher modes are important, these simplified approximation methods cannot accurately estimate the seismic deformation demands and nonlinear time history analysis should be used. In such situation, in order to avoid high computational intensity, model reduction methods can be used. For many civil engineering structures, the large numbers of degrees of freedom are dictated by their topology, rather than by the expected complexity of the response. Therefore, by eliminating undesirable degrees of freedom and meeting desirable ones, computational cost can be reduced. The methods for reducing the degrees of freedom have been referred to as model reduction methods or condensation methods. Reviewing the literature of model reduction methods is out of the scope of this study, and can be found in [3].

It should be noted that condensed models are also very useful for researchers who want to simulate the behavior of structures when subjected to a large number of earthquake records to allow for the inherent randomness and uncertainties of ground motions. From the review of the literature [4–6] it is observed that such investigations were generally conducted on a few representative structures rather than many sample structures having various structural configurations and geometrical and material properties. It is a compromise between the amount of information required for statistical quantification and the time needed for nonlinear time history analyses of the detailed structures.

¹ Department of Civil Engineering, Fars Science and Research Branch, Islamic Azad University, Fars, Iran

² Department of Civil Engineering, Shiraz Branch, Islamic Azad University, Shiraz, Iran

* Corresponding author, email: ashkan.sha@gmail.com

In the field of civil engineering, seismic researchers and engineers have been widely used equivalent single degree of freedom (SDOF) systems as a condensed model for the estimation of global seismic deformation demand of structures [1, 2, 7–9]. In these approaches, the equivalent nonlinear static analysis is used to estimate local deformation demands. The accuracy of these methods is directly related to the assumptions and associated uncertainties which are made to convert the detailed model to an equivalent SDOF system and to convert global deformations into local deformations.

Several multi degrees of freedom (MDOF) condensed models are also developed and are extensively used by researchers for seismic response prediction of structures [10–16]. Equivalent “shear beam” and “shear frame” models are the MDOF condensed models that were traditionally used to reduce computational intensity. The accuracy of these two condensed models has been evaluated by Diaz et al. [17]. They concluded that the equivalent shear beam model produces results clearly different from those of its original frame counterpart. The ductility demands for middle floors obtained from the analysis of shear-frame model are much less than those obtained from the analysis of original frame counterpart. For shear-frame model, ductility demands are concentrated at the lowest floor and top floor. Thus, these condensed models have not enough accuracy for estimation of seismic demands.

Another condensed model which is used for analysis of MRF structures is commonly known as fish-bone (FB) model. In the FB model, at every floor level, all columns of the original frame are replaced by a single column, and all beams are replaced by two beams with a roller support as shown in Fig. 1b. The model allows beam plastic hinges and story mechanisms to develop as much as they can in the original frame (Fig. 1a).

Nakashima et al. [18] by evaluating the FB model developed a simplified generic frame (GF) model to simulate the seismic response of steel moment frames. The GF model consists of a single column with rotational spring at every floor level as shown in Fig. 1c. The underlying assumption for this model is that all rotations at joints lying at each floor level are identical, and axial elongation and contraction of beams and columns are also neglected. Nakashima et al. [18] concluded the accuracy of the GF model is good for most regular moment frames. However, for tall frames, overall flexural deformation caused by axial deformations of columns becomes significant and cannot be considered in the GF model because the axial deformation of columns is ignored in this model. Another shortcoming of the GF model is due to the assumption of equal rotation at each story joints, which can produce large errors for frames with irregular member arrangements.

In 2013, FB model modified by Khaloo and Khosravi [19] through three enhancements: (i) in order to consider flexural deformation of moment frames due to axial elongation and contraction of columns, a number of truss elements are added

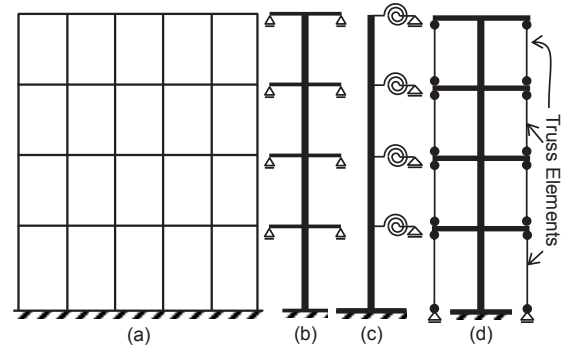


Fig. 1 a) Original moment resisting frame, b) fish-bone Model, c) generic frame model, d) modified fish-bone model

to the fish-bone model as shown in Fig. 1d, (ii) the moment of inertia for beams is slightly reduced to modify the assumption of equal rotation at each floor level joints, and (iii) in order to consider simultaneous yielding at both ends of the beam in original moment frames, moment-rotation relation of rotational springs is supposed to be bilinear instead of trilinear. The adequacy of this model is evaluated with respect to nonlinear dynamic analysis results of three 5-, 10- and 20-story regular moment resisting frames subjected to 94 records; and it is concluded that the modified fish-bone (MFB) model is evidently more precise than the original fish-bone model.

Although among the physically condensed model available in the literature, MFB model is potentially the best for regular MRF, the adequacy of this model should be evaluated for irregular MRF structures. For frames with irregular member arrangements and span, plastic hinge rotations for beams (and columns) lying at each story level are not identical, which may produce large errors.

In this paper, after a few modifications to the MFB model formulation for irregular frames, the adequacy of the model is evaluated for irregular MRF structures. These irregularities include mass, stiffness and strength irregularity in the height of frames as well as in member arrangements and span of each story level. The effects of ductility demand and frame height on the accuracy of the MFB model are also investigated. Finally, two simple and effective procedures are suggested to improve the MFB models.

2 Modified Fish-Bone model for Irregular MRF

As Mentioned Previously, the MFB model is a condensed model for MRF structures, which can provide a nonlinear response of these structures with much lower computational intensity. To achieve a fish-bone model through an Original MRF, the following assumptions are adopted:

1. Mass is lumped at floor levels.
2. All rotations at interior joints lying at each floor level are identical, and rotations at exterior joints are somewhat more (the rotations of two exterior joints are identical).
3. Axial forces of interior columns due to lateral forces are negligible and the story overturning moment sustained by two exterior columns.

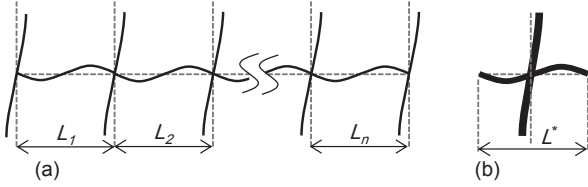


Fig. 2 Conversion of MRF to MFB model: a) MRF b) MFB model

Based on the assumption (2), all columns in each story can be condensed into one representative column, and all beams at each floor level can also be condensed into two half-beams (see Fig. 1d). Thus, the plastic moment capacity of the representative column (\tilde{M}_{pc}) should be equal to the sum of the plastic moment capacity (M_{pc}) for all columns in the story under consideration and the stiffness of the representative column should be equal to the sum of the stiffness for all columns in the corresponding story. Since the height of all columns located in each story are identical and equals to the height of the corresponding representative column, the effective flexural stiffness of the cross-section of the representative column (\tilde{EI}_c) can be considered as the sum of the effective flexural stiffness (EI_c) for all columns in the corresponding story.

The plastic moment capacity of each representative half-beam (\tilde{M}_{pb}) should also be equal to the sum of the plastic moment capacities (M_{pb}) of individual beams at the floor under consideration. The effective flexural stiffness of the cross-section of the two half-beam (\tilde{EI}_b) for MFB model at each floor should be determined in such a way that their participation in the lateral stiffness of the corresponding story is equivalent to the participation of the original frame beams for the story (The same lateral elastic displacement for both models when subjected to the same shear story forces). This can be done using slope-deflection equation as follows.

Referring to Fig. 2, the left end moments of beams of MRF are as follows:

$$\begin{cases} M_1^L = \frac{2E_1I_1}{L_1}(2\alpha\theta + \theta) \\ \vdots \\ M_i^L = \frac{2E_iI_i}{L_i}(2\theta + \theta) \\ \vdots \\ M_n^L = \frac{2E_nI_n}{L_n}(2\theta + \alpha\theta) \end{cases} \quad (1)$$

where M_1^L and M_n^L are the left end moments for two exterior beams, M_i^L is the left end moments for i -th interior beam, θ is the rotation of interior joints, α is the ratio of exterior joint rotation to interior joint rotation which is obtained easily through a linear static pushover analysis of the MRF. The value of α is not dependent on the lateral load [19]. E , I and L are Young's modulus, moment of inertia and length of beams, respectively.

Summing both sides of Eqs. (1), the slope-deflection relationship for right half-beam of MFB model is obtained as

$$\sum_{i=1}^n M_i^L = 2 \left[(2\alpha + 1) \frac{E_1I_1}{L_1} + 3 \sum_{i=2}^{n-1} \frac{E_iI_i}{L_i} + (2 + \alpha) \frac{E_nI_n}{L_n} \right] \theta \quad (2)$$

where n is the number of bays. The above equation relates the whole bending moment to the interior joints rotation θ . The mean value of rotation (θ_m) at each floor level is calculated as

$$\theta_m = \frac{(n-1)\theta + 2\alpha\theta}{n+1} = \frac{2\alpha + n-1}{n+1} \theta \quad (3)$$

Substituting θ_m for θ in Eq. (2), the following slope-deflection relationship is derived for the right half-beam of the MFB model:

$$\sum_{i=1}^n M_i^L = \tilde{K} \theta_m \quad (4)$$

in which \tilde{K} is the stiffness of the representative right half-beam of the MFB model, and is calculated as

$$\tilde{K} = \frac{2(n+1)}{2\alpha + n-1} \left[(2\alpha + 1) \frac{E_1I_1}{L_1} + 3 \sum_{i=2}^{n-1} \frac{E_iI_i}{L_i} + (2 + \alpha) \frac{E_nI_n}{L_n} \right] \quad (5)$$

The stiffness of the representative left half-beam also requires similar calculation and achieves exactly the same results. If the length of each half-beam of the MFB model is selected as $L^*/2$ (see Fig. 2b), the effective flexural stiffness of the cross-section of the representative half-beams (\tilde{EI}_b) can be obtained using slope-deflection method as $\tilde{EI}_b = \tilde{K}L^*/6$. Thus

$$\tilde{EI}_b = \frac{(n+1)L^*}{6\alpha + 3n-3} \left[(2\alpha + 1) \frac{E_1I_1}{L_1} + 3 \sum_{i=2}^{n-1} \frac{E_iI_i}{L_i} + (2 + \alpha) \frac{E_nI_n}{L_n} \right] \quad (6)$$

For fully regular frames with equal span length in which EI/L is identical for all beams lying at each floor, Eq. (6) can be simplified as that developed by Khaloo and Khosravi [19]

$$\tilde{EI}_b = \left[n - \frac{(n-1)(\alpha-1)}{n+1+2(\alpha-1)} \right] EI_b \quad (7)$$

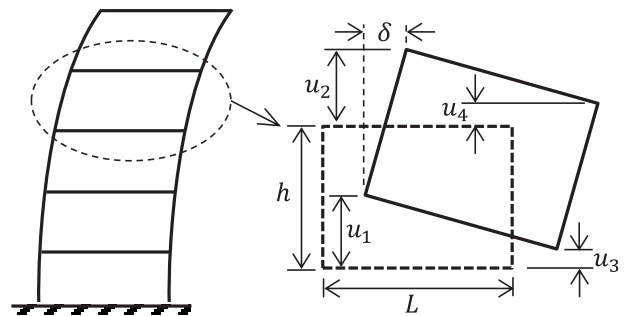


Fig. 3 Vertical displacement components for the definition of flexural drift

Based on the assumption (3), the flexural deformation of MRF can be taken into account by inserting a pair of truss elements at each story of MFB model (see Fig. 1d). The axial stiffness of the truss elements of each story should be calculated in such a way that the flexural inter-story drift in the MFB model becomes equal to the flexural inter-story drift in the MRF.

Referring to Fig. 3, the flexural inter-story drift at each story can be obtained as

$$\delta = \frac{h}{2L}(u_1 + u_2 - u_3 - u_4) \quad (8)$$

where u_1, u_2, u_3 and u_4 are vertical displacements of exterior joints at each story. h and L are the height of the story and the distance between the exterior columns, respectively. The derivation of Eq. (8) is described in detail in [20]. Thus, the flexural inter-story drift at each story for MRF and MFB model are determined by Eqs. (9) and (10), respectively.

$$\delta = \frac{h}{2\sum L_i}(u_1 + u_2 - u_3 - u_4) \quad (9)$$

$$\tilde{\delta} = \frac{h}{2L^*}(\bar{u}_1 + \bar{u}_2 - \bar{u}_3 - \bar{u}_4) \quad (10)$$

where $\sum L_i$ is the distance between the exterior columns of MRF and L^* is the distance between the pair of truss elements at each story of MFB model.

The vertical displacement of each exterior joint of MRF (i.e. u_1, u_2, u_3 and u_4) at floor level "m" equals the sum of elongation (or contraction) for all columns below this joint which can be calculated by [19]

$$u_{1,4} = \sum_{i=1}^m \frac{P_i h_i}{(EA)_i} \quad (11)$$

where P_i, h_i and $(EA)_i$ are the axial force, height and axial stiffness of the cross-section of the exterior column at story i , respectively. As mentioned previously, the story overturning moment due to lateral loads is sustained by two exterior columns in the MRF and a pair of truss elements in the corresponding MFB at each story. Since this story overturning moment is identical for both models, the axial forces of the truss elements of the MFB are " β " times greater than those of the exterior columns of MRF ($\beta = \sum L_i / L^*$). Thus, the vertical displacement at exterior joints of the MFB model (i.e. $\tilde{u}_1, \tilde{u}_2, \tilde{u}_3$ and \tilde{u}_4) at floor level "m" can be expressed as

$$\tilde{u}_{1,4} = \sum_{i=1}^m \frac{\beta P_i h_i}{(\widetilde{EA})_i} \quad (12)$$

in which P_i and h_i equals the same parameters in Eq. (11), but the axial stiffness of the cross-section of the truss elements $(\widetilde{EA})_i$ should be calculated so that it produces the same flexural inter-story drift as in the corresponding MRF. By equating Eqs. (9) and (10):

$$\begin{aligned} \delta = \tilde{\delta} \rightarrow u_{1,4} &= \left(\frac{\sum L_i}{L^*} \right) \tilde{u}_{1,4} \rightarrow \sum_{i=1}^m \frac{P_i h_i}{(EA)_i} = \beta \sum_{i=1}^m \frac{\beta P_i h_i}{(\widetilde{EA})_i} \\ \Rightarrow (\widetilde{EA})_i &= \beta^2 (EA)_i \end{aligned} \quad (13)$$

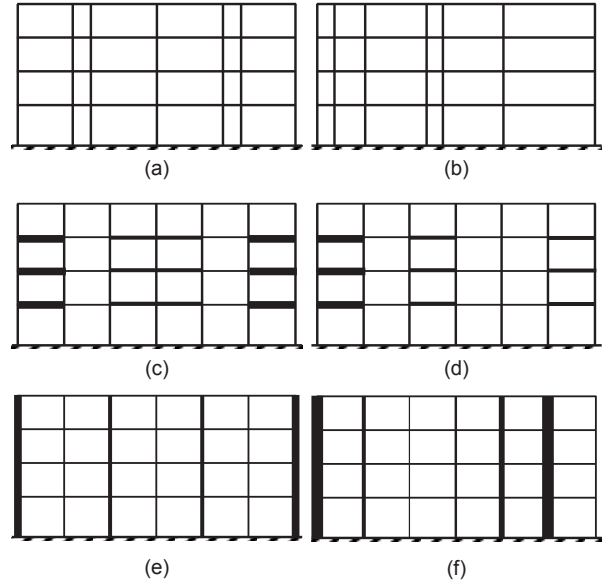


Fig. 4 Schematic representations of frames for the definition of irregularities

Briefly, the axial stiffness of the cross-section of each truss element in the MFB model should be " β^2 " times greater than the axial stiffness of the cross-section of the corresponding exterior column in the MRF ($\beta = \sum L_i / L^*$).

3 Frame models

To evaluate the accuracy of the MFB model for irregular frames, two regular frames (F0-4 and F0-7) and eighteen irregular frames with the following irregularities were selected.

- Two symmetrical frames (F1-4 & F1-7) with span length irregularity for adjacent spans (Fig 4a).
- Two unsymmetrical frames (F2-4 & F2-7) with span length irregularity for adjacent spans (Fig 4b).
- Two symmetrical frames (F3-4 & F3-7) with stiffness and strength irregularity for adjacent beams (Fig 4c).
- Two unsymmetrical frames (F4-4 & F4-7) with stiffness and strength irregularity for adjacent beams (Fig 4d).
- Two symmetrical frames (F5-4 & F5-7) with stiffness and strength irregularity for adjacent columns (Fig 4e).
- Two unsymmetrical frames (F6-4 & F6-7) with stiffness and strength irregularity for adjacent columns (Fig 4f).
- Two frames with vertical mass irregularity (F7-4 & F7-7).
- Two frames (F8-4 & F8-7) with horizontal mass irregularity (mass irregularity for adjacent spans).
- Two fully irregular frames (F9-4 & F9-7) with respect to span length, member strength and stiffness arrangements, horizontal and vertical mass.

The above frames are 4- and 7-story steel moment resisting frames in which the story height is 3 m. The load resisting systems for 4- and 7-story frames are respectively 6- and 4-bay with variable span length (between 2 and 6 m). More details of these frames are not presented here for the sake of space consideration. For more information, one can refer to [21].

Table 1 First three natural periods of models

Frame	Mode 1		Mode 2		Mode 3	
	MRF	MFB	MRF	MFB	MRF	MFB
F0-4	0.734	0.744	0.217	0.225	0.119	0.119
F1-4	0.673	0.623	0.200	0.193	0.110	0.107
F2-4	0.830	0.824	0.224	0.250	0.133	0.132
F3-4	0.729	0.733	0.216	0.233	0.119	0.119
F4-4	0.687	0.690	0.206	0.213	0.116	0.116
F5-4	0.804	0.802	0.244	0.249	0.138	0.136
F6-4	0.753	0.754	0.223	0.229	0.123	0.122
F7-4	0.778	0.795	0.254	0.263	0.123	0.119
F8-4	0.598	0.604	0.178	0.183	0.097	0.097
F9-4	0.724	0.691	0.209	0.207	0.111	0.108
F0-7	1.320	1.321	0.419	0.419	0.230	0.230
F1-7	1.370	1.363	0.428	0.428	0.231	0.232
F2-7	1.348	1.300	0.421	0.410	0.227	0.224
F3-7	1.314	1.290	0.416	0.410	0.228	0.226
F4-7	1.230	1.210	0.392	0.386	0.217	0.216
F5-7	1.337	1.311	0.422	0.413	0.230	0.226
F6-7	1.375	1.355	0.437	0.431	0.242	0.238
F7-7	1.271	1.272	0.401	0.401	0.222	0.222
F8-7	1.506	1.506	0.478	0.477	0.263	0.263
F9-7	1.274	1.153	0.397	0.368	0.213	0.205

For each of the aforementioned MRF, the corresponding MFB model was generated. All of these MRF and their MFB counterparts were analyzed using OpenSEES software [22] in which second-order P-Delta effect is considered. Both of the models are simulated using nonlinear beam-column elements with fiber section in which nonlinear stress-strain relationship is assigned to the material behavior.

For these frames, the calculated natural periods are between 0.59s and 1.51s. The first three calculated periods for these models are summarized in Table 1. It can be seen that the periods of the MFB model are close to the periods of the corresponding original MRF. The maximum error is 9.5% for the fully irregular 7-story frame (F9-7). It seems that the accuracy of the MFB model is more affected by the span length irregularity than the other irregularity.

Table 2 Main properties of the considered ground motions

Earthquake Name	Year	Station	Magnitude	Mechanism	Rjb (km)	Rrup (km)	V_{s30} (m/s)	PEER Seq. #
Palm Spring	1986	San Jacinto -Soboba	6.06	Reverse Oblique	22.96	23.31	447.22	534
Cape Mendocino	1992	Cape Mendocino	7.01	Reverse	0	6.96	567.78	825
Tabas	1978	Tabas City	7.35	Reverse	1.79	2.05	766.77	143
Northridge	1994	Santa Monica City Hall	6.69	Reverse	53.94	57.67	322	1014
IMPV	1979	Delta	5.01	strike slip	49.4	49.93	242.05	196
Kobe	1995	Sakai	6.9	strike slip	28.08	28.08	256	1115
Hollister	1961	Hollister City Hall	5.6	strike slip	19.55	19.56	198.77	26
El Centro	1940	Borrego Valley	6.9	strike slip	32.44	34.98	213.44	4

Rjb: Joyner-Boore distance to rupture plane

Rrup: Closest distance to rupture plane

4 Earthquake ground motions

In order to investigate the accuracy of the MFB model for irregular MRF structures, eight far-field earthquake ground motions were selected from the strong ground motion database of the Pacific Earthquake Engineering Research (PEER) Centre (<http://ngawest2.berkeley.edu/site>).

To ensure that the MRF respond into the intermediate and high inelastic range when subjected to ground motions, each record was scaled to two PGA. Records with smaller PGA (I-PGA) were used to produce intermediate demand ductility in the models while records with greater PGA (H-PGA) were used to produce high demand ductility in the models. It should be mentioned that the I-PGA and H-PGA vary for different frames. The main properties of the considered Earthquake ground motions are summarized in Table 2.

5 Evaluation of MFB Method

In order to evaluate the accuracy of the MFB, nonlinear time history analysis was performed for all MRF and MFB models. For each MRF subjected to each record, peak inter-story drift ratio, over time, for each story (ID_i) is determined as exact inter-story drift demand. The corresponding predicted inter-story drift (\widetilde{ID}_i) is also determined for MFB models. The results computed from each MRF were compared to the results obtained from the corresponding MFB model.

For each MRF and the corresponding MFB model subjected to each record the following error measures were computed:

$$e_i = \left(\frac{\widetilde{ID}_i}{ID_i} - 1 \right) \times 100 \quad (14)$$

$$Err = \sqrt{\frac{1}{n} \sum_{i=1}^n e_i^2} \quad (15)$$

Where n is the number of stories. e_i is a local error at a given level i for a frame model while Err defines a global error for the frame. Since the structural damage is directly related to local deformations, Eq. (14) is important from the design point of view. If the e_i is negative, the MFB underestimates the inter-story drift; but $e_i > 0$ means the MFB overestimates the inter-story drift.

Fig. 5a compares the average of e_i for different 4-story frame models subjected to the record groups with I-PGA intensity. In these cases the demand ductility varies between 2.0 and 2.7 for different frame models. It can be seen that the MFB model overestimates the inter-story drift of regular frame model (frame F0-4) in average, but it may overestimate or underestimate the inter-story drift of irregular frame models. Fig. 5b compares the average of e_i for different 4-story frame models subjected to the record groups with H-PGA intensity. In these cases the demand ductility varies between 4.0 and 4.6 for different frame models. It can be observed that, except for the case of span length irregularities, the MFB model overestimates the inter-story drift of lower stories and underestimate the inter-story drift of upper stories.

Fig. 5c and Fig. 5d illustrate Err together with period errors for different 4-story frame models. The period error is calculated as the absolute difference of unity and the ratio of the natural period computed via MFB to the exact one calculated from MRF ($|1 - T_{MFB}/T_{MRF}|$). As one can notice, increasing the period error leads to increasing Err and vice versa. This issue can be used to estimate the error level of the results obtained from the MFB model.

Another point to be noted from Fig. 5c and Fig. 5d is that, except for the cases of span length irregularities, the MFB is not sensitive to other irregularities and it can predict the inter-story drift of these irregular frame models as well as the regular frames. However, in the case of span length irregularities, the local and global errors are limited to 30% and 22%, respectively. Also, the accuracy of the MFB is not significantly sensitive to the ductility demand.

Fig. 6a compares the average of e_i for different 7-story frame models subjected to the record groups with I-PGA intensity. For these cases the demand ductility varies between 2.0 and 2.2 for different frame models. The comparison of e_i for different 7-story frame models subjected to the record groups with H-PGA intensity is shown in Fig. 6b. In these cases, the demand ductility varies between 4.1 and 4.5 for different frame models. It can be seen that the MFB model may overestimate or underestimate the inter-story drift of frame models.

Fig. 6c and Fig. 6d illustrate Err together with period errors for different 7-story frame models. Again, it can be observed that by increasing period error, Err is also increased and vice versa. For this group of frame models, the maximum errors are

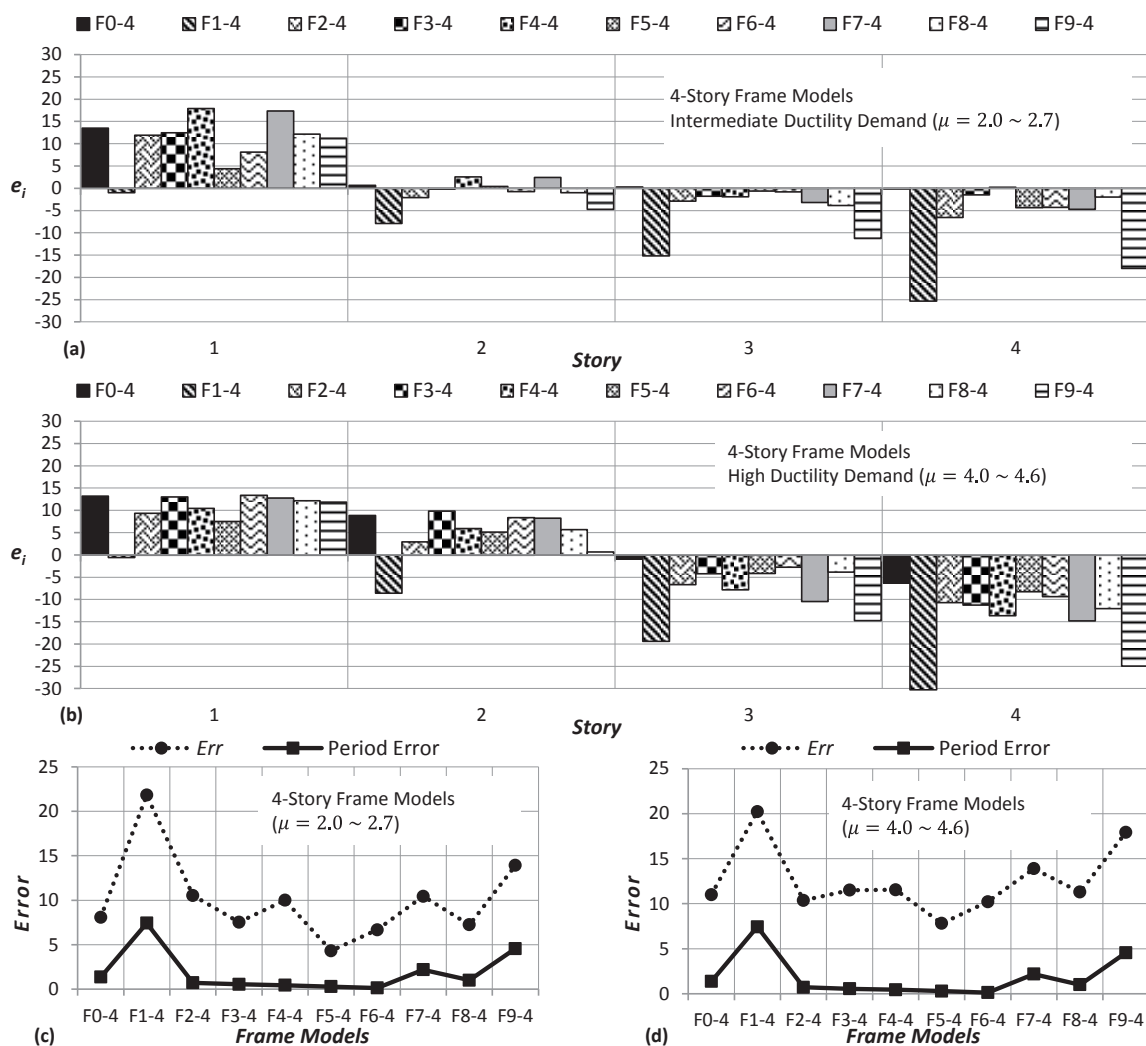


Fig. 5 Error measures for 4-story frames: a) average of e_i for I-PGA, b) average of e_i for H-PGA, c) average of Err for I-PGA and d) average of Err for H-PGA

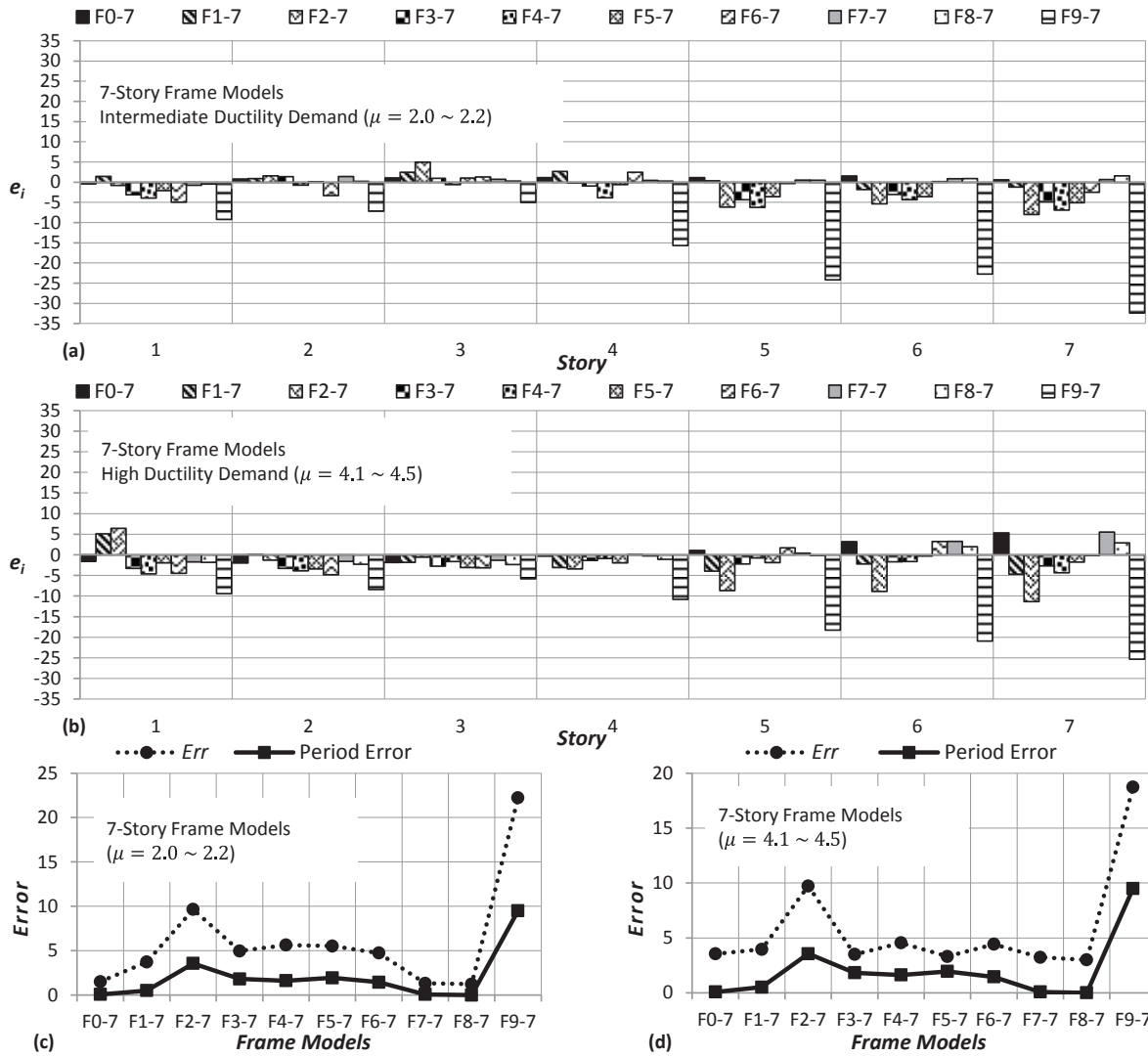


Fig. 6 Error measures for 7-story frames: a) average of e_i for I-PGA, b) average of e_i for H-PGA, c) average of Err for I-PGA and d) average of Err for H-PGA

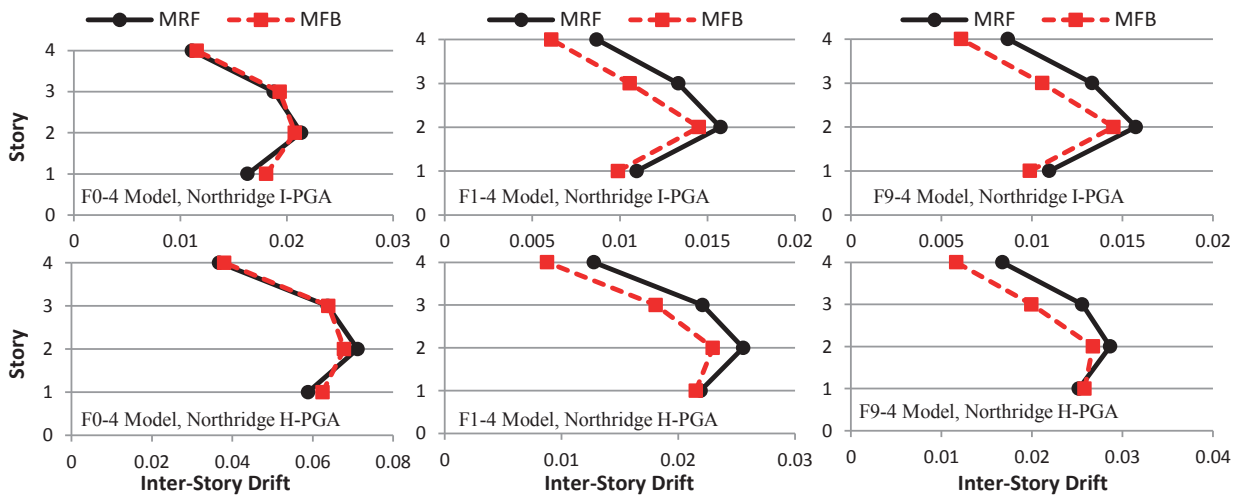


Fig. 7 Inter-story drift distribution along the building height for different 4-story frame models subjected to Northridge earthquake

related to fully irregular frame model and the local and global errors are limited to 32% and 22%, respectively. For other 7-story frame models, the local and global errors are less than 10%. Again, it can be seen that the accuracy of the MFB is not significantly sensitive to the ductility demand. It is observed

that the MFB model was more accurate for 7-story frame models than 4-story frame models.

Several examples of inter-story drift distribution along the building height for frame models subjected to special ground motions are shown in Fig. 7 and Fig. 8.

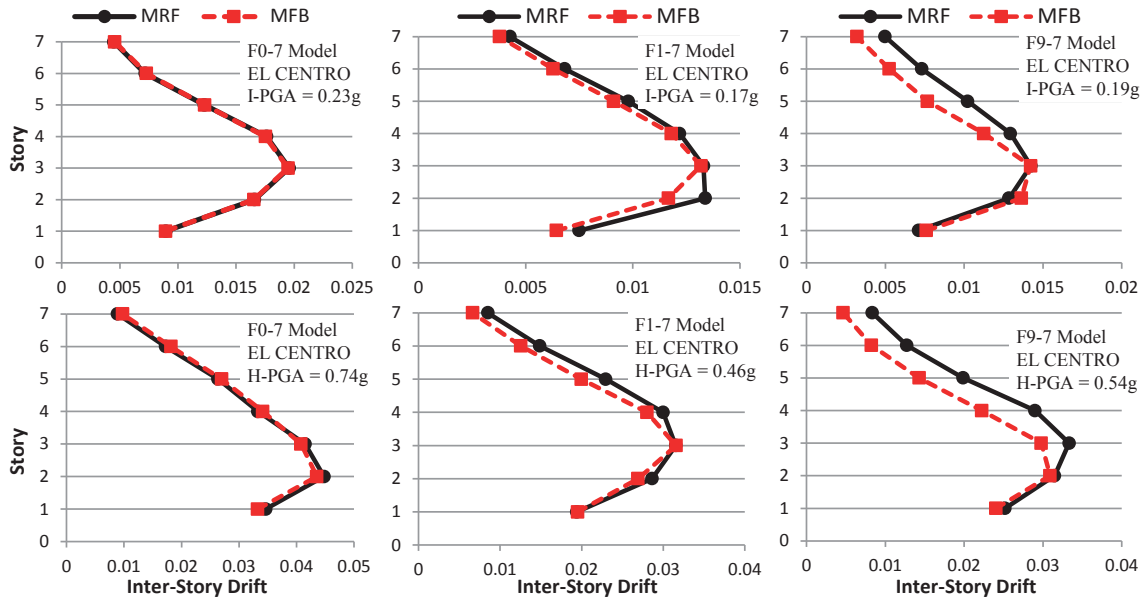


Fig. 8 Inter-story drift distribution along the building height for different 7-story frame models subjected to El Centro earthquake

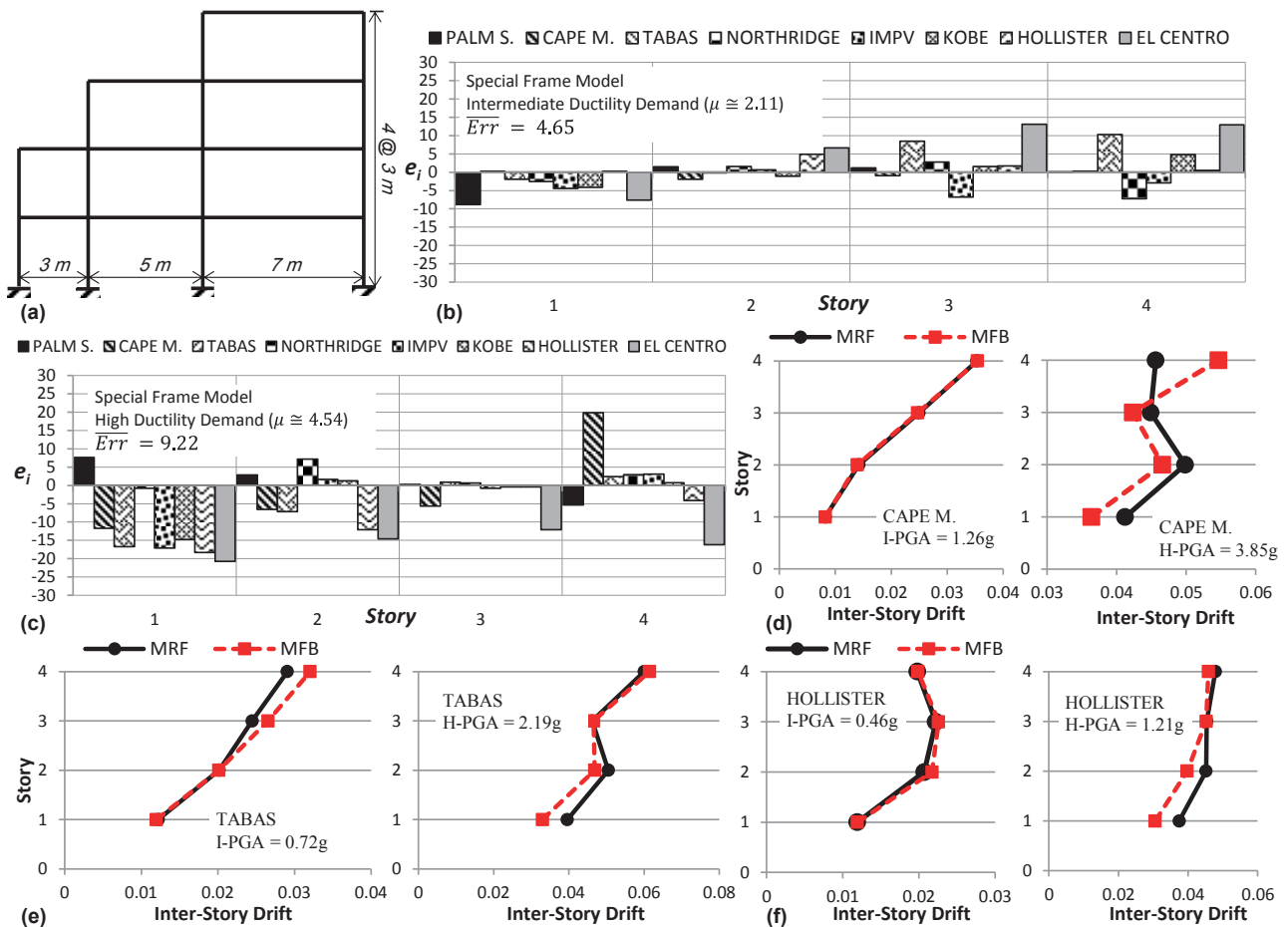


Fig. 9 Results of the special irregular frame model subjected to different ground motions

The analysis results of a special frame model with setback irregularity are illustrated in Fig. 9. The configuration of this frame model is shown in Fig 9a. The first three periods of MRF model are 0.787, 0.293 and 0.135 seconds and the first three periods of corresponding MFB model are 0.781, 0.285 and 0.128 seconds. The errors e_i for different earthquake ground motions with I-PGA and H-PGA intensity are shown in Fig.

9b and Fig. 9c, respectively. It can be observed that the MFB model may overestimates or underestimate the inter-story drift of the frame model. For intermediate and high ductility demand, the errors are limited to 13% and 21%, respectively. Fig. 9d through Fig. 9f present several examples of inter-story drift distribution along the frame model height for different ground motions.

6 Improving MFB models

As observed in the previous section, in some cases MFB models exhibit significantly different results than the corresponding original frames (especially for span length irregularities). Obviously, this error is due to the simplified assumptions that are used to create the MFB model. Some of these assumptions are not suitable for irregular models. It is clear that the MFB model can be improved by considering compatibility conditions for members and more complex assumptions. But it should be borne in mind that if the calculations used to make the MFB model complicated, then the reason for using this model (simplifying and reducing computational intensity) has been questioned and the user would prefer to use the original MRF model instead of using this model.

In the previous section, it is observed that the accuracy of the inter-story drift prediction is related to the period error. Increasing the period error results in more error in the nonlinear analysis result and vice versa. This idea can be used to improve the MFB model. Due to the fact that the modal parameters of each system are dependent on the members' stiffness of that system, it is possible to modify the modal parameters of the system by modifying the members' stiffness of the system.

It is possible to modify the members' stiffness of the MFB model by performing an optimization process in such a way that the modal parameters of the MFB model approach enough to the modal parameters of the original MRF model. However, it should be remembered that providing a sophisticated optimization process for improving the MFB model will make the modified model lose its simplicity.

In this section, two simple systematic procedures are introduced to reduce the period errors for improving MFB models. In the first procedure, a modification factor is used to modify the flexural stiffness of all members of the MFB so that the natural period of the MFB model approaches the natural period of the corresponding original MRF. In the second procedure, a modification factor is only used to modify the flexural stiffness of half-beams of the MFB model in such a way that the natural period of the MFB model approaches the natural period of the corresponding original MRF. The second procedure is an iterative approach.

Regarding the relationship between period and stiffness of a system ($T = 2\pi\sqrt{m/K}$), the modification factor, γ , can be calculated as follows

$$\frac{T_1}{T_2} = \frac{2\pi\sqrt{\frac{m}{K_1}}}{2\pi\sqrt{\frac{m}{K_2}}} \rightarrow K_2 = \left(\frac{T_1}{T_2}\right)^2 K_1 \rightarrow \gamma = \left(\frac{T_1}{T_2}\right)^2 \quad (16)$$

The above equation states that for a system with a natural period of T_1 and a stiffness of K_1 , to change the natural period of the system to T_2 , the stiffness of the system should be modified by multiplying the modification factor $\gamma = (T_1/T_2)^2$.

6.1 Procedure #1

In this procedure, the improved MFB model is generated with the following steps:

1. Generate the initial MFB model based on the formulation provided in section 2.
2. Perform a modal analysis to determine the natural period of vibration for the original MRF model (T_{MRF}) and the corresponding initial MFB model (T_{MFB}).
3. Generate improved MFB model by modifying the flexural stiffness of all members (half-beams and columns) of the Initial MFB via multiplying the modification factor $\gamma = (T_{MFB}/T_{MRF})^2$.

It should be noted that if T_{MFB} is sufficiently close to T_{MRF} , then there is no need to improve the Initial MFB model.

6.2 Procedure #2

The details of this procedure are expressed as a sequence of the following steps:

1. Generate the MFB model based on the formulation provided in section 2.
2. Perform a modal analysis to determine the natural period of vibration for the original MRF model (T_{MRF}) and the corresponding MFB model (T_{MFB}).
3. Modify the MFB model via multiplying the flexural stiffness of all half-beams only (i.e. not columns) of the MFB by the modification factor $\gamma = (T_{MFB}/T_{MRF})^2$.
4. Perform a modal analysis to determine the natural period of vibration for the new MFB model (T_{MFB}).
5. If the period error ($|1 - T_{MFB}/T_{MRF}|$) is greater than a predefined threshold, repeat steps 3 to 5 to reduce the period error for improving MFB model.

It should be noted that if T_{MFB} for initial MFB model is sufficiently close to T_{MRF} , then there is no need to improve the Initial MFB model.

To evaluate the efficiency of these procedures let us consider the F9-7 model with the period error of 9.5%. For this frame model, *Err* is 22.21% and 18.73% for intermediate and high ductility demand, respectively. The corresponding MFB model was improved by the above mentioned procedures. For the improved MFB model via procedure #1 (Imp. MFB #1), the period error was reduced to 0.16%. With this modification *Err* was reduced by at least about 40% to 12.90% and 10.35% for intermediate and high ductility demand, respectively. For the improved MFB model via procedure #2 (Imp. MFB #2), the period error was reduced to 0.31% in the third iteration. This modification led to a better accuracy of the nonlinear analysis results. *Err* was reduced by about 60% to 9.33% and 7.57% respectively for intermediate and high ductility demand.

The comparison of e_i for initial MFB, improved MFB via procedure #1 (Imp. MFB #1) and improved MFB via procedure #2 (Imp. MFB #2) is shown in Fig. 10. It can be observed that the procedure #2 is more accurate than the procedure #1.

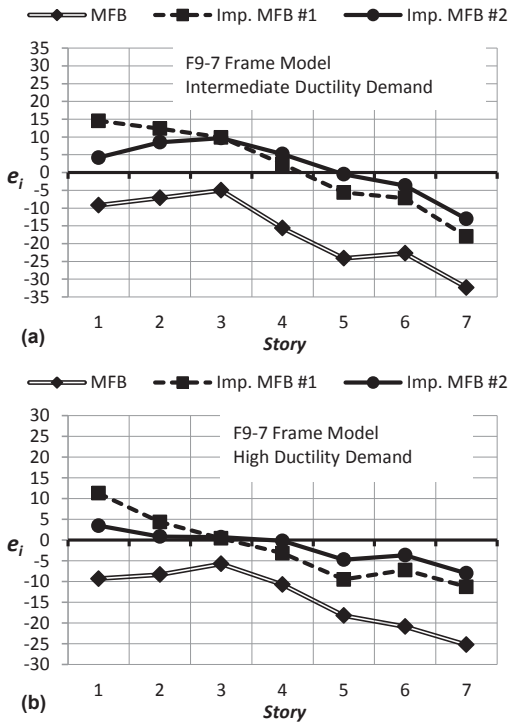


Fig. 10 Average of e_i for MFB and improved MFB of F9-7 frame model.

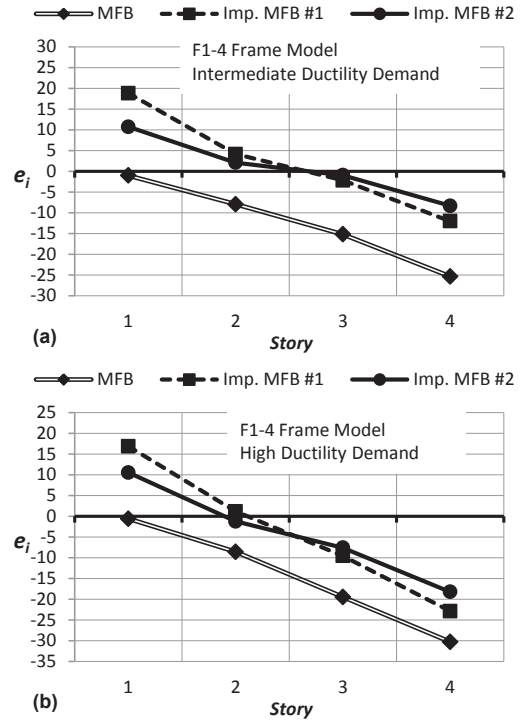


Fig. 11 Average of e_i for MFB and improved MFB of F1-4 frame model.

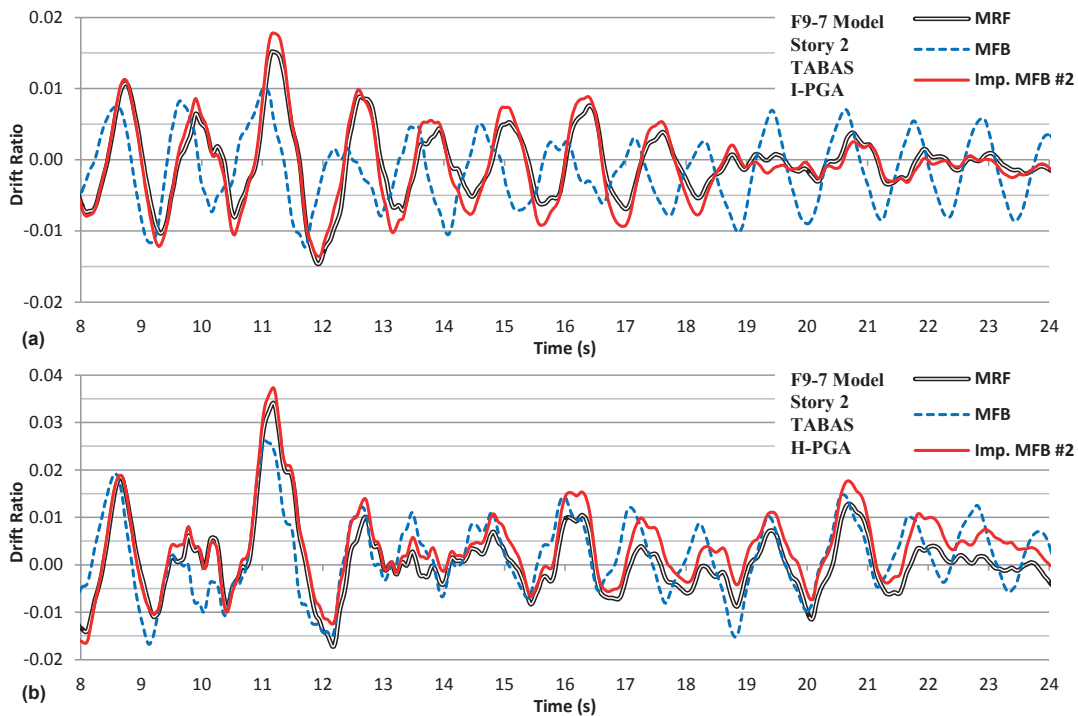


Fig. 12 Inter-story drift time history of the second story of F9-7 model subjected to Tabas record: a) intermediate and b) high demand ductility.

As a second example, these procedures are used to improve the corresponding MFB model of F1-4 frame. For the improved MFB model via procedure #1, the period error was reduced from 7.43% to 0.30%. With this modification Err was reduced from 21.81% and 20.23% to 12.49% and 15.29% for intermediate and high ductility demand, respectively. For the improved MFB model via procedure #2, the period error was reduced to 0.45% in the third iteration. Again this modification led to

a better accuracy of the nonlinear analysis results. Err was reduced to 8.53% and 11.42% for intermediate and high ductility demand, respectively. Fig. 11 compares the average of Err for initial MFB, improved MFB via procedure #1 (Imp. MFB #1) and improved MFB via procedure #2 (Imp. MFB #2) of F1-4 frame model.

Fig. 12 present inter-story drift time history for the second story of the F9-7 model subjected to the Tabas ground motion

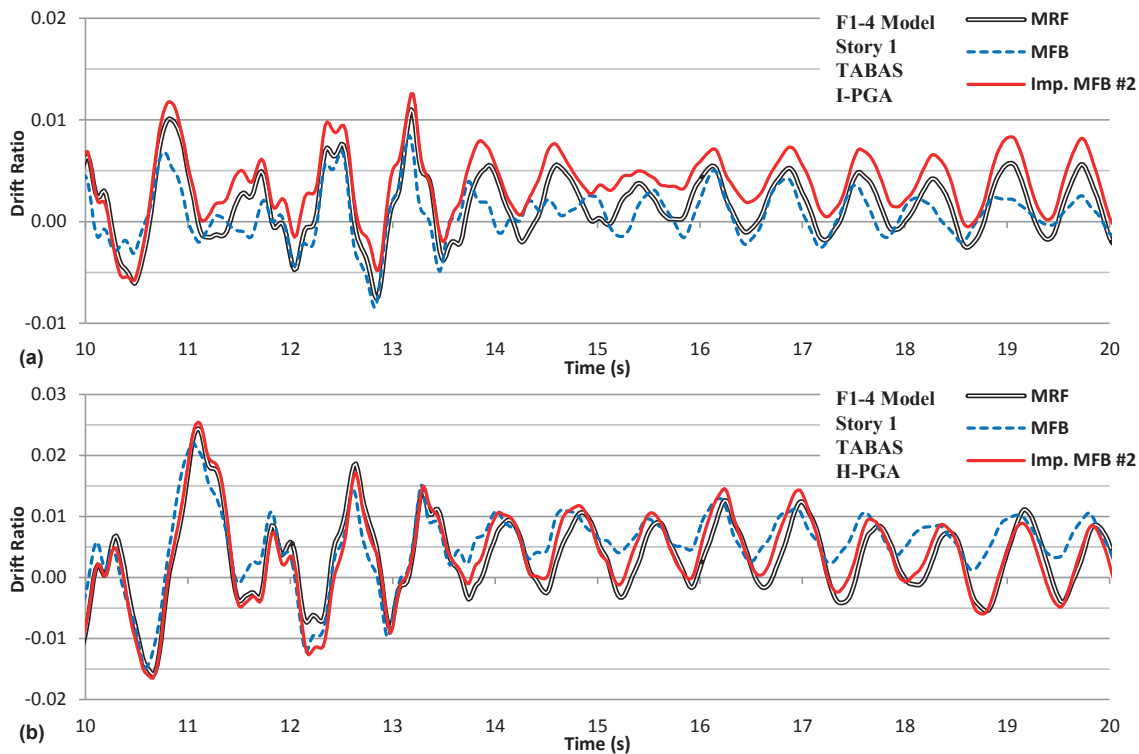


Fig. 13 Inter-story drift time history of the first story of F1-4 model subjected to Tabas record: a) intermediate and b) high demand ductility.

record that compares the variation of inter-story drift for original MRF with the corresponding MFB and improved MFB models. For the sake of clarity, only the results for 8 to 24 seconds are shown in the figure. It is clearly evident that the improved MFB model response closely matches the original MRF but the MFB model response exhibits great differences in amplitude and frequency.

Inter-story drift time histories for the first story of the F1-4 models subjected to the Tabas ground motion record are shown in Fig. 13. For clarity, only the results for 10 to 20 seconds are presented in the figure. It can be seen that the results obtained from the Improved MFB models are more accurate than those obtained from the MFB models. Moreover, the variation of inter-story drift over time for the improved MFB model is much more similar to the MRF (Figs. 12 and 13). It should be noted that the inter-story drift time histories obtained from the improved model via procedure #1 (Imp. MFB #1) are very similar to those obtained from the improved model via procedure #2 (Imp. MFB #2) and not presented here for the sake of space consideration. However, it can be said that the improved model via the procedure #2 is slightly better than the improved model via the procedure #1.

Based on the above observation, it is very useful to check the modal properties of the MFB model before running the nonlinear time history analysis. As the modal properties (i.e. natural period) of the MFB model are closer to those of the original MRF, the nonlinear time history analysis results will be more accurate. If necessary, the MFB model can be improved by one of the above-mentioned procedures.

7 Summary and conclusions

The accuracy of the Modified Fish-Bone (MFB) model to estimate the maximum inter-story drift demands of irregular moment resisting frame structures was evaluated. To do this, a few modifications were made to the MFB model formulation and then two regular and nineteen irregular frames with different irregularities were selected. The nonlinear time history analysis was performed for each detailed frame (MRF) and the corresponding MFB model subjected to two earthquake record groups: one group with I-PGA intensity that produced intermediate ductility demand ($\mu = 2.0 \sim 2.7$) in the models and the other with H-PGA that produced high ductility demand ($\mu = 4.0 \sim 4.6$) in the models. Two error measures (local and global) were defined and these were compared for frames with different irregularities. Finally, two simple and effective procedures are suggested to improve the MFB models. This investigation has led to the following conclusions:

- Among the different irregularities, the MFB model is more affected by the span length irregularity.
- Except for the cases of span length irregularities, the MFB is not sensitive to other irregularities and it can predict the inter-story drift of these irregular frame structures as well as the regular frame structures.
- The MFB model may overestimates or underestimates the inter-story drift of frame structures.
- The accuracy of MFB model is not significantly sensitive to the ductility demand.
- It seems that the MFB model is more accurate for high rise frame structures than low rise frame structures.

- The accuracy of MFB model to predict the inter-story drift ratio is related to the modal properties of the MFB Model. As the modal properties of the MFB model are closer to those of the original MRF, the nonlinear time history analysis results will be more accurate.
- If the modal properties of the MFB model (such as natural periods) deviate from those of the original MRF, the MFB model can be improved by one of the two simple and effective procedures introduced in this paper. This improvement will lead to a better accuracy of nonlinear analysis results.

References

- [1] ASCE. "FEMA 356: Prestandard and Commentary for the Seismic Rehabilitation of Building". Rehabilitation 519. Washington, D.C., USA: Federal Emergency Management Agency (FEMA). 2000. Retrieved from <https://www.fema.gov/media-library/assets/documents/757>
- [2] ASCE. "ASCE/SEI 41-13: Seismic Evaluation and Retrofit of Existing Buildings". Reston, Virginia, USA: American Society of Civil Engineers. 2014. <https://doi.org/10.1061/9780784412855>
- [3] Noor, A. K. "Recent advances and applications of reduction methods". *Applied Mechanics Reviews*, 47(5), pp. 125. 1994. <https://doi.org/10.1115/1.3111075>
- [4] Gupta, A., Krawinkler, H. "Behavior of Ductile SMRFs at Various Seismic Hazard Levels". *Journal of Structural Engineering*, 126(1), pp. 98–107. 2000. [https://doi.org/10.1061/\(ASCE\)0733-9445\(2000\)126:1\(98\)](https://doi.org/10.1061/(ASCE)0733-9445(2000)126:1(98))
- [5] Lin, Y.-Y., Miranda, E. "Estimation of Maximum Roof Displacement Demands in Regular Multistory Buildings". *Journal of Engineering Mechanics*, 136(1), pp. 1–11. 2010. [https://doi.org/10.1061/\(ASCE\)0733-9399\(2010\)136:1\(1\)](https://doi.org/10.1061/(ASCE)0733-9399(2010)136:1(1))
- [6] Erduran, E., Kunnath, S. K. "Enhanced Displacement Coefficient Method for Degrading Multi-Degree-of-Freedom Systems". *Earthquake Spectra*, 26(2), pp. 311–326. 2010. <https://doi.org/10.1193/1.3381157>
- [7] Applied Technology Council. "FEMA 440: Improvement of Nonlinear Static Seismic Analysis Procedures". Redwood City, California, USA: Federal Emergency Management Agency (FEMA). 2005. Retrieved from <https://www.fema.gov/media-library/assets/documents/855>
- [8] Akkar, S. D., Miranda, E. "Statistical evaluation of approximate methods for estimating maximum deformation demands on existing structures". *Journal of Structural Engineering*, 131(1), pp. 160–172. 2005. [https://doi.org/10.1061/\(ASCE\)0733-9445\(2005\)131:1\(160\)](https://doi.org/10.1061/(ASCE)0733-9445(2005)131:1(160))
- [9] Ruiz-García, J. "Inelastic Displacement Ratios for Seismic Assessment of Structures Subjected to Forward-Directivity Near-Fault Ground Motions". *Journal of Earthquake Engineering*, 15(3), pp. 449–468. 2011. <https://doi.org/10.1080/13632469.2010.498560>
- [10] Miranda, E. "Approximate Seismic Lateral Deformation Demands in Multistory Buildings". *Journal of Structural Engineering*, 125(4), pp. 417–425. 1999. [https://doi.org/10.1061/\(ASCE\)0733-9445\(1999\)125:4\(417\)](https://doi.org/10.1061/(ASCE)0733-9445(1999)125:4(417))
- [11] Miranda, E., Reyes, C. J. "Approximate lateral drift demands in multi-story buildings with nonuniform stiffness". *Journal of Structural Engineering*, 128(7), pp. 840–849. 2002. [https://doi.org/10.1061/\(ASCE\)0733-9445\(2002\)128:7\(840\)](https://doi.org/10.1061/(ASCE)0733-9445(2002)128:7(840))
- [12] Miranda, E., Akkar, S. D. "Generalized Interstory Drift Spectrum". *Journal of Structural Engineering*, 132(6), pp. 840–852. 2006. [https://doi.org/10.1061/\(ASCE\)0733-9445\(2006\)132:6\(840\)](https://doi.org/10.1061/(ASCE)0733-9445(2006)132:6(840))
- [13] Hajirasouliha, I., Doostan, A. "A simplified model for seismic response prediction of concentrically braced frames". *Advances in Engineering Software*, 41(3), pp. 497–505. 2010. <https://doi.org/10.1016/j.advengsoft.2009.10.008>
- [14] Kuang, J. S., Huang, K. "Simplified multi-degree-of-freedom model for estimation of seismic response of regular wall-frame structures". *The Structural Design of Tall and Special Buildings*, 20(3), pp. 418–432. 2011. <https://doi.org/10.1002/tal.538>
- [15] Huang, C.-T. "Considerations of Multimode Structural Response for Near-Field Earthquakes". *Journal of Engineering Mechanics*, 129(4), pp. 458–467. 2003. [https://doi.org/10.1061/\(ASCE\)0733-9399\(2003\)129:4\(458\)](https://doi.org/10.1061/(ASCE)0733-9399(2003)129:4(458))
- [16] Khaloo, A. R., Khosravi, H. "Multi-mode response of shear and flexural buildings to pulse-type ground motions in near-field earthquakes". *Journal of Earthquake Engineering*, 12(4), pp. 616–630. 2008. <https://doi.org/10.1080/13632460701513132>
- [17] Diaz, O., Mendoza, E., Esteva, L. "Seismic ductility demands predicted by alternate models of building frames". *Earthquake Spectra*, 10(3), pp. 465–487. 1994. <https://doi.org/10.1193/1.1585785>
- [18] Nakashima, M., Ogawa, K., Inoue, K. "Generic frame model for simulation of earthquake responses of steel moment frames". *Earthquake Engineering & Structural Dynamics*, 31(3), pp. 671–692. 2002. <https://doi.org/10.1002/eqe.148>
- [19] Khaloo, A. R., Khosravi, H. "Modified fish-bone model: A simplified MDOF model for simulation of seismic responses of moment resisting frames". *Soil Dynamics and Earthquake Engineering*, 55, pp. 195–210. 2013. <https://doi.org/10.1016/j.soildyn.2013.09.013>
- [20] Moghaddam, H., Hajirasouliha, I., Doostan, A. "Optimum seismic design of concentrically braced steel frames: concepts and design procedures". *Journal of Constructional Steel Research*, 61(2), pp. 151–166. 2005. <https://doi.org/10.1016/j.jcsr.2004.08.002>
- [21] Haghight, A. "Estimation of Seismic Demand Rotation of Plastic Hinges of Moment Resisting Frames Using Nonlinear Dynamic Analysis of Condensed Models". Islamic Azad University, Shiraz Branch. 2017.
- [22] OpenSEES Team. "Open System for earthquake engineering simulation". Berkeley: Pacific Earthquake Engineering Research center, University of California. 2017. Retrieved from <http://opensees.berkeley.edu/>